Étude expérimentale et numérique d'un implant de hanche en composite CFRP: Analyse par thermographie IR

Habiba Bougherara, Ehsan Ur Rahim, Suraj Shah, Lotfi Toubal, Redouane Zitoune

Étude expérimentale et numérique d'un implant de hanche en composite CFRP: Analyse par thermographie IR

Experimental and numerical study of composite CFRP hip implant: thermography analysis

Habiba Bougherara[1], Ehsan Ur Rahim[1], Suraj Shah[1], Lotfi Toubal[2] and Redouane Zitoune[3]

1: Department of Mechanical and Industrial Engineering
Ryerson University – Toronto, ON M4C 5M6, Canada
2: Department of Mechanical Engineering
Université du Québec à Trois-Rivières, QC G9A 5H7, Canada
3: Institut Clément Ader (ICA) Groupe
Matériaux et Structures Composites 133, 31077 Toulouse cedex 4
e-mail : habiba. bougherara@ryerson.ca, erahim@ryerson.ca, suraj.shah@ryerson.ca, Lotfi.Toubal@uqtr.ca, Redouane.Zitoune@iut-tlse3.fr

Résumé

Une utilisation de plus en plus importante des matériaux composites dans les applications orthopédiques, nous oblige à améliorer nos évaluations des niveaux des contraintes afin d'éviter toute défaillance prématurée des implants. En biomécanique, les chercheurs utilisent des jauges de déformation pour mesurer les déformations à différents endroits de l'implant et les résultats sont utilisés pour valider expérimentalement les modèles éléments finis. Notre travail présente et valide une nouvelle technique basée sur des mesures non destructives. La thermographie infrarouge a été utilisée pour étudier les cartographies des contraintes d'une prothèse en composite avec des fibres de carbone et une matrice polyamide (CF/PA12). Les résultats montrent une bonne corrélation entre les mesures réalisées avec la thermographie IR et ceux obtenus par des jauges de déformation. Cette étude est une première étape pour valider la technique IR dans les applications en biomécanique.

Abstract

With the resurgence of composite materials in orthopaedic applications, a rigorous assessment of stress is needed to quantify stress shielding and avoid any premature failure of bone-implant systems. For current biomechanics research, strain gauge measurements are employed to experimentally validate finite element models, which then characterize stress in the bone and implant. Our study introduces and validates a new non-destructive testing technique for orthopaedic implants. Lock-in infrared (IR) thermography validated with strain gauge measurements was used to investigate the stress and strain patterns in a novel composite hip implant made of carbon fibre reinforced polyamide 12 (CF/PA12). Results showed almost perfect agreement of IR thermography versus strain gauge data with a Pearson correlation of $R^2 = 0.96$ and a slope = 1.01 for the line of best fit. IR thermography detected hip implant peak stresses on the inferior-medial side just distal to the neck region of 31.14 MPa (at 840 N), 72.16 MPa (at 1500 N), and 119.86 MPa (at 2100 N). This is the first study to experimentally validate and demonstrate the applicability of lock-in IR thermography to obtain three-dimensional stress field in a biomechanics application.

Mots Clés : Biomécanique,thermographie infrarouge, contrainte, déformation, prothèse composite
Keywords : biomechanics; infrared thermography; stress; strain; composite hip implant.

1. Introduction

Metallic hip implants are much stiffer than bone and, thus, carry a higher proportion of the load during weight bearing or other activities. Known as "stress shielding", this abnormal load sharing has been linked to bone loss and implant loosening around the bone-implant interface in total hip replacements [1-2]. This is a major concern for hip replacement surgery patients and is particularly acute in elderly patients suffering from osteoporosis or osteoarthritis. Thus, adequate in-vitro characterization of stress in the bone and the implant is required.
To overcome stress shielding by increasing load transfer to the bone, research has been done on different combinations of low stiffness materials to find an appropriate candidate for total hip arthroplasty [3-6]. Biocomposites are an attractive solution for orthopaedic implants due to their

tailored mechanical properties, biocompatibility, and mechanical reliability [7]. A carbon fibre reinforced polyether-ether-ketone (CF/PEEK) hip stem was introduced by Akay and Aslan [3]. The authors claimed that the CF/PEEK reduced the stress in the implant compared to conventional titanium and cobalt-chrome implants. Another concept design of a hybrid hip prosthesis was developed by Simões and Marques [4] which is based on a cobalt-chrome core with an outer layer made of a flexible composite. They demonstrated that the combination of a stiff material with a more flexible one produced the desired load transfer distribution. More recently, Bougherara et al. [5-6] developed a biomimetic composite made of 68% carbon fibre and 32% nylon that had similar properties to cortical bone. They showed that an optimum load transfer and a maximum stability could be achieved using this material [5-6,8-9].

The aforementioned studies have mechanically assessed the strain in a few locations on the surface of the composite implants using strain gauge measurements. Typically, the strain gauge tests are then used to validate finite element models, which are employed to generate three dimensional stress fields of the hip implants to understand the biomechanics more fully [10]. However, although strain gauges are considered a "gold standard" in biomechanical studies, they have several important drawbacks. Strain gauges are not accurate near high peak stress points, provide only an average value at a given position, cannot give full three-dimensional stress maps, are physically fragile, and have a finite size that limits where they can be placed on the surface of an implant. To avoid these disadvantages and to eliminate the need for the second step of developing a finite element model for more thorough stress analysis, a new non-destructive validated experimental technique needs to be developed for use in biomechanics applications. Only two prior studies used infrared (IR) thermography to investigate surface stress fields in biomechanics applications [11-12]. However, neither of these reports experimentally validated the thermographic technology with another well-accepted experimental technique.

Therefore, our study experimentally validated and then used a novel IR thermography method to record the full three-dimensional stress maps of a composite hip implant undergoing cyclic axial loading. Specifically, we used strain gauges to measure strains on the surface of the composite hip implant and compared the results to those obtained using an IR camera. This is the first study to experimentally validate and then demonstrate the applicability of this IR thermography to assess stresses in a biomechanics application.

2. Methods

2.1 General Approach

A polymer composite hip implant was instrumented with strain gauges and mechanically tested using average axial cyclic forces of 840 N, 1500 N, and 2100 N. The hip implant was then retested mechanically without strain gauges under the same load regimes while a three-dimensional surface stress map was obtained using an IR thermography technique. Strain values were compared between the two techniques. The findings have practical implications for the hip implant's clinical performance and the potential applicability to biomechanics of the IR thermography method.

2.2 Strain Gauge Experiments

The hip implant used presently was employed in prior investigations by some of the authors [5-6] (Fig. 1). It was made of a 3-mm thick substructure of CF/PA12 (carbon fibre reinforced polyamide 12). The implant has a textured surface due to the orientation of the woven fibres, a hollow oval cross-section, a 135° shaft angle, a 3-mm wall thickness, a 230-mm overall length, a 30.3-mm maximum diameter at the proximal base of the neck, a 37.5 mm offset, and a 15.8-mm minimum diameter at the distal tip. A metal ball was mounted onto the proximal tip to simulate a femoral head.

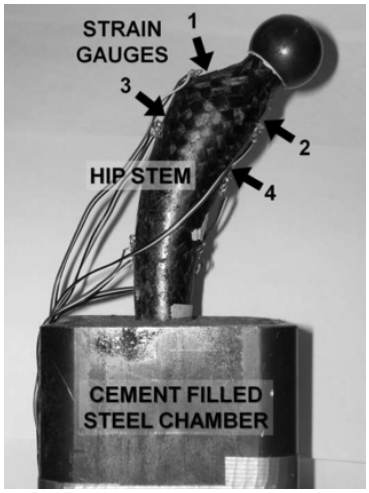

Fig. 1. Composite hip implant instrumented with strain gauges and fixed in a cement-filled steel chamber.

The hip implant was cemented into a square-channel steel chamber. The implant was first mounted onto a chemistry stand using an adjustable multi-axial clamp. The lateral surface was then aligned vertically using leveling gauges. The distal tip was lowered into the centre of a hollow square-channel steel chamber (88 mm wide X 88 mm wide X 160 mm high). Anchoring cement (Flow-Stone, King Packaged Materials Company, Burlington, ON, Canada) was poured into the square potting chamber until it was filled to the brim. The cement dried 24 hours prior to the specimen being removed from the clamping system. The resulting working length of the hip implant from the top of the potting chambers to the top of the femoral ball was 115 mm.
The hip implant was then instrumented with four Vishay® 350-Ohm general-purpose uniaxial linear pattern gauges (125UW, model CEA-06-125UW-350, Vishay Micro-Measurements & SR-4, Raleigh, NC, USA). Wire leads were soldered to the gauges, secured to the implant using electrical tape, and attached to an 8-channel Cronos-PL data acquisition system (IMC Mess Systeme GmbH, Berlin, Germany). This system was interfaced to a computer for data storage and analysis using FAMOS V5.0 software (IMC Mess-Systeme GmbH, Berlin, Germany).

The hip implant was then distally secured to the base of a mechanical tester using an industrial vice at an adduction angle of 15 deg to simulate the single-legged stance phase of walking gait (Fig. 2).

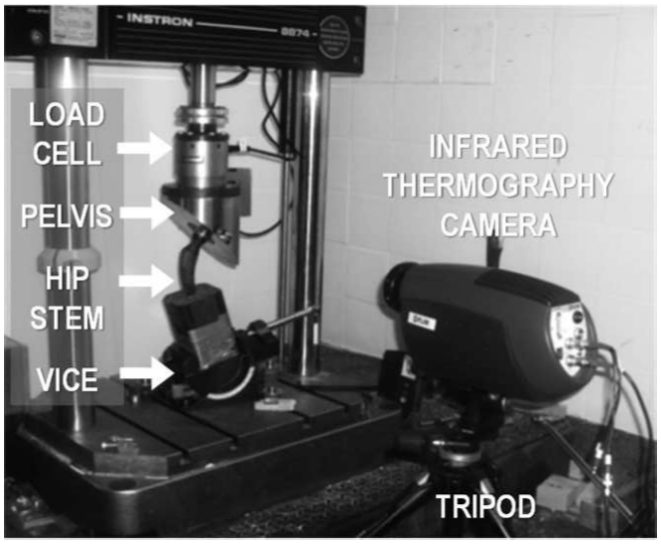

Fig. 2. Experimental setup used for mechanical cyclic testing of the composite hip implant.

A stainless steel load applicator shaped like a pelvic cup applied a 100 N preload to the femoral ball to prevent slippage between the pelvic cup and the femoral ball. Using displacement control, a vertical cyclic force (average, 840 N; range, 460 to 1360 N) was imposed on the implant at 5 Hz for a minimum of 120 s to allow the specimen to reach a constant force level prior to strain gauge data collection. The frequency was chosen to match and accommodate the requirements of the IR thermography testing described below. The waveform was sinusoidal to mimic human walking gait on the hip joint [13]. Force and displacement from the load cell were recorded every 0.01 s. Surface strain gauge data were collected and averaged for 30 s during mechanical loading. Tests were repeated with average loads of 1500 N (range, 630 to 2580 N) and 2100 N (range, 600 to 3820 N). These forces represented 1.2, 2.2, and 3.1 times body weight for a 70 kg person, which are in the range of clinical hip joint forces [13]. Force versus displacement graphs for all tests showed almost perfect linear behaviour with an average Pearson coefficient of $R^2 = 0.98$, indicating the implant was within the linear elastic region and incurred no permanent damage during experimentation. Hooke's law was finally used to calculate surface stresses by multiplying the strain gauge values by the modulus of elasticity of the composite material (E = 14.5 GPa).
An Instron 8874 mechanical tester (Instron Corp., Norwood, MA, USA) was used to generate the force regimes on the hip implant for all experiments. The load cell had a linear capacity of ±25 kN, a resolution of 0.1 N, and an accuracy of ±0.5%. The mechanical tester had a stiffness of 260 kN/mm, which was much higher than the 2 kN/mm stiffness of the current composite hip implant [6]. Thus, no correction factor was necessary to accommodate for mechanical tester compliance. Experiments were done at 22°C ambient temperature.

2.3 Infrared (IR) Thermography Experiments

The IR thermal camera used in this study was a Silver 420 (FLIR Systems Canada, Burlington, ON, Canada). It had an image resolution of 1 MPa, an image size of 320 X 256 pixels, a built-in auto focusing 27 mm lens, and a 5 Hz to 170 Hz frame rate. It senses surface temperature changes on an object due to the object's cyclic vibration at a fixed frequency to which the camera has been synchronized, being referred to as "lock-in". The camera then uses dedicated software called Altair-Li (Cedip Infrared Systems, Croissy-Beaubourg, France) to convert changes in surface temperature to surface stresses using user-inputted parameters.
The operating principle of the IR camera is as follows. The synchronizing or "lock-in" system obtains four signal values S1, S2, S3, and S4 in every pixel of the image at four different times, from which is calculated a phase value $\Phi = \arctan[(S1-S3)/(S2-S4)]$. Using Φ, the system produces a phase image. Thermo-elastic stress analysis is based on the principle that when a body is compressed, its temperature increases. When the pressure is released, it returns to its original shape and temperature. The thermo-elastic equation used by the IR camera to generate stress fields is :

$$\Delta\sigma = \Delta T \, \rho \, C / (\alpha \, T), \qquad \text{(Eq. 1)}$$

where ΔT is the temperature change sensed by the camera, ρ is the material density, C is the specific heat capacity, α is the coefficient of thermal expansion, and T is the ambient temperature sensed by the camera. This equation assumes adiabatic conditions, i.e. no significant heat loss. The values inputted into the software for the composite hip implant material were ρ = 1.43 g/cm3, C = 485 J/(kgK), and $\alpha = 7.64\ 10\text{-}6° \ C^{-1}$ [8]. The mechanical test setup was done in the same manner as described earlier for strain gauge experiments (Fig. 2). The only difference was that there were no strain gauges attached to the implant. The IR camera was mounted on a tripod and placed 91 cm from the hip implant, ensuring that the hip implant was located in the middle of the image window. The camera recorded the oscillating surface temperature of the object by taking a series of images in which every pixel represented the average temperature of the matching location. The camera generated stress maps while averaging the applied force on the sinusoidal waveform. Similar test

setups were used previously to image a metallic hip implant inserted into a synthetic femur and a synthetic femur on its own [11-12].

3. Results

3.1. IR thermography validation

Results of the IR thermographic surfaces stresses versus strain gauge stresses for locations 1 to 4 are shown (Fig. 3). There was a strong correlation between these two experimental techniques, yielding a high Pearson coefficient of R2 = 0.96 and a slope = 1.01. This was close to perfect correlation, which would have given R2 = 1 and slope = 1.

3.2. IR Thermography Stress Maps

Thermographic stress maps for the hip implant are shown (Fig. 4). Stresses extracted from the images are also given (Tab. 1). Similar images were obtained for the 840 N, 1500 N, and 2100 N axial force tests. Maximum surface stresses on the hip implant were 31.14 MPa (at 840 N), 72.16 MPa (at 1500 N), and 119.86 MPa (at 2100 N), which were all on the medial side just distal to the neck region. Excluding peak values, the mean stresses and their standard deviations on the rest of the implant were 3.00 +/- 3.15 MPa (at 840 N), 5.41 +/- 6.80 MPa (at 1500 N), and 10.50 +/- 12.43 MPa (at 2100 N).

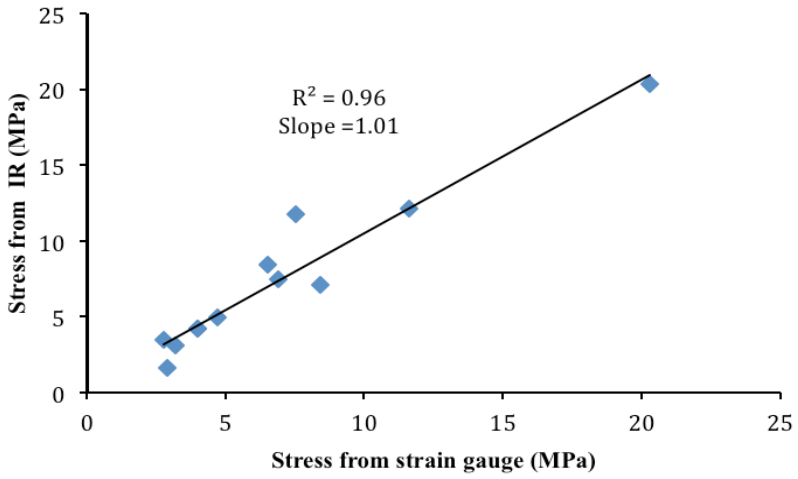

Fig. 3. Correlation graph of surfaces stresses from IR thermography versus strain gauges.

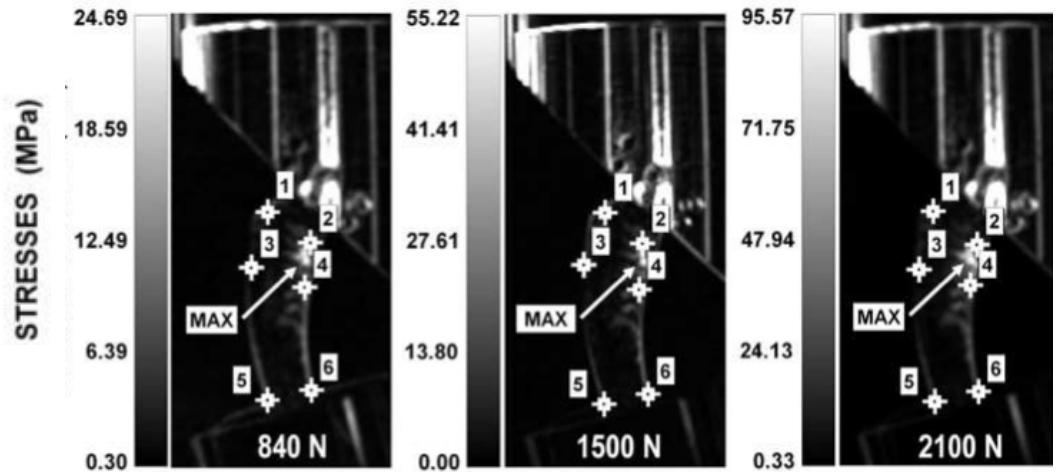

Fig. 4. IR thermography grayscale images of three-dimensional surface stresses on the composite hip implant for the three cyclic force levels

Hip stem location	Stress (MPa) Axial force			Pearson Correlation R^2
	840 N	1500 N	2100 N	
1	3.50	4.19	8.44	0.83
2	7.10	12.09	20.33	0.97
3	1.58	4.21	7.46	0.99
4	3.10	4.97	11.73	0.89
5	1.41	1.54	2.11	0.87
6	1.52	1.60	2.26	0.81
Max	31.14	72.16	119.86	0.95
Mean	3.00 (3.15)	5.41 (6.80)	10.50 (12.43)	

Tab. 2. Le module de Young, les contraintes et les déformations à la rupture pour les éprouvettes fibres de chanvre avec et sans papiers.

4. Discussion

4.1. General findings

Lock-in IR thermography was employed for the non-destructive assessment of a polymer composite hip implant. The method permitted full three-dimensional surface stress maps to be generated. Results were validated experimentally with strain gauge measurements. The hip implant itself had high peak stresses distal to the neck region and is a site for potential failure. Surface stresses increased in direct proportion to the axial cyclic load level applied. This is the first study which has experimentally validated and used this lock-in IR thermography technology to evaluate an orthopaedic implant device.

4.2. Comparison of Present Results to Prior Studies

Several prior investigations evaluated surface stress and strain of metallic and polymer-based composite hip implants, whose results can be compared to our findings. Any differences are due to variations in material properties, hip implant geometry, hip implant alone versus hip implant inserted into a femur, mechanical test setup, force levels applied, static versus cyclic forces, etc. Akay and Aslan [3] used a CF/PEEK composite implant (E = 16.4 GPa) inserted into a synthetic femur and subjected it to a static 3000 N load at a 20 deg adduction angle. Six strain gauges were placed on the lateral site of the implant, and five gauges were on the medial side. The maximum lateral tensile stress on the implant was about 40 MPa, and the maximum medial compressive stress was about 60 MPa. Our medial compressive stresses were also higher than our lateral tensile stresses. However, our maximum stress was 119.86 MPa at a cyclic axial force of 2100 N applied at 15 deg of adduction, being much higher than the previous study.

Bougherara et al. [5] conducted finite element analysis on a titanium-based alloy (E = 110 GPa) and a CF/PA12 (E = 14.5 GPa) composite hip implant both inserted into a femur. A static axial load of 3000 N was applied at an adduction angle of 20 deg. Peak stress was 79 MPa for the titanium implant and 72 MPa for the composite implant. Bone resorption and implant loosening could be minimized if the composite hip implant was used. Our maximum stress of 72.16 MPa when using a

1500 N cyclic force was similar to the prior report, but it was much higher at 119.86 MPa when a 2100 N cyclic force was applied.

Bougherara et al. [6] developed a strain gauge validated finite element model of a CF/PA12 composite hip implant alone that was not inserted into a femur. The implant was subjected to a static axial load of 3000 N at an adduction angle of 0 deg. Our stress patterns on lateral and medial was similar to this prior study, i.e., tension on the lateral side and compression on the medial side with a peak value in the neck region. However, our peak stress value of 119.86 MPa at a cyclic axial force of 2100 N was much higher than their 68.9 MPa value.

Helgason et al. [14] used finite element analysis to assess the risk of implant failure during walking gait. The implant was made from titanium alloy (E = 110 GPa). They set the value of failure to 493 MPa of stress. Static forces were applied in the range of 803 N to 1014 N. A maximum stress of 47.2 MPa was present around the implant on the outer posterior surface of the bone at the proximal end of the implant, whereas a 61.5 MPa stress was found in the proximal part of the diaphysis. Our maximum stresses were 31.14 MPa (at 840 N) and 72.16 MPa (at 1500 N), being similar to the prior study for a comparable load range.

Regarding IR themography, only two prior studies have sued this technology to evaluate surface stress fields in biomechanics applications. Zanetti and coworkers examined surface stresses on an intact synthetic femur alone subjected to cyclic forces ranging from 300 N to 1300 N at 10 Hz [11]. Hyodo and colleagues assessed a metallic hip implant inserted into a synthetic femur, oriented in 9° of adduction, and subjected it to 5 Hz of cyclic loading ranging from 300 N +/- 200 N to 1800 N +/- 1700 N [12]. However, neither of these reports experimentally validated their thermographic results with another well-accepted experimental stress or strain measurement technique, as was done presently with strain gauges.

4.3. Practical Implications

Stress values measured using IR thermography almost perfectly agreed with surface strain gauges (Fig. 3). This technology, therefore, can be successfully used for quality assurance testing of orthopaedic implants undergoing cyclic loading. The method's pros and cons should be noted with respect to orthopaedic applications [6, 10, 15]. Firstly, IR thermography gives a three-dimensional stress map of the test specimen surface. This eliminates the need to develop and validate finite element models commonly used in biomechanical research. Secondly, IR thermography is non-destructive and does not damage surface features of the test specimen. Once experimentally validated, there is no need to mount strain gauges to the surfaces of subsequent specimens, as often done in biomechanical studies. Thirdly, IR thermography needs test specimens to undergo cyclic loading to generate a temperature map that is converted to a stress map. This coincides with real-life clinical conditions that orthopaedic prostheses experience, namely, cyclic loading [13, 16]. Fourthly, IR thermography is a relatively easy "point and shoot" method that only requires minimal preparation of the test setup. However, IR thermography also has cons. Image quality can be compromised due to test specimen surface texturing, which may not allow some orthopaedic devices to be assessed properly because of the presence of surface roughening elements which promote clinical bone ongrowth [15]. A minimum 3 to 5 Hz loading frequency is required to generate enough cyclic surface temperature gradient on the test specimen which can be synchronized to the IR camera. Stress maps cannot be generated for one times events like the impact failure of a prosthesis or bone-implant construct [16-19], since this does not produce a cyclic temperature gradient which can be synchronized to the IR camera. The high purchase price of an IR thermography system can be prohibitive for some researchers.

Peak stress occurred in the proximal neck region of the hip implant (Fig. 4). This zone would be particularly susceptible to failure if the implant were inserted into a human femur in vivo and subjected to physiological loading conditions over a long period of time. This potential failure site

has also been detected by Bougherara et al. in a prior finite element model validated by experiments [6]. They assessed the same composite hip implant by experimentally and virtually mounted it into a rigid block, which represented a femur of excellent bone quality and perfect bony ongrowth. They reported a finite element peak stress of 68.9 MPa in the inferior neck region of the composite hip implant and only slightly lower stress levels just distal to this area. As such, it is proposed that the good bone stock of a healthy human femur could provide rigid fixation which would allow high stress to develop in the composite hip implant's neck region, predisposing it to potential failure. Conversely, the poor bone stock arising from severe osteopenia or osteoporosis may not permit the composite hip implant to be anchored firmly, thereby causing the site of implant failure, loosening, or migration to occur in the distal region where the implant is in direct contact with the bone. To prove these hypotheses, future in vitro biomechanical tests need to be done in which the composite hip implant is mounted in a synthetic or human femur mimicking high and low quality bone stock.

Proximal surface stresses (i.e. locations 1 to 4 and the “max” point) were high and strongly correlated with axial cyclic force level, whereas distal surface stresses (i.e. locations 5 and 6) remained low as force increased (Tab. 1). Thus, an implant recipient’s body weight or activity level will directly influence the amount of stress generated in the proximal portion of a hip implant, but will not necessarily affect stresses in the distal portion where the device is anchored firmly in the femur bone. This assumes, of course, that the implant insertion point provides adequate rigid fixation for the implant via good bony ongrowth or good quality bone stock, as provided presently with the cement block. This coincides with the findings reported in prior finite element and experimental studies on composite and metallic hip implants used in primary or revision hip replacement surgery [6, 15]. This also agrees with the common clinical recommendations given to hip implant recipients, namely, that heavier patients should lower their body weight and that younger active patients should minimize high impact activities.

4.4. Limitations

Despite the following drawbacks, this is the first investigation to experimentally validate this lock-in IR thermography technique for any orthopaedic biomechanics application and the first to use the method to assess the performance of a composite implant. Cyclic loads were applied within the linear elastic region of the composite material of the hip implant and only for a limited number of cycles. This avoided any permanent damage to the implant, so that testing at all three load levels could be completed. Cyclic forces, however, should be considered to understand more comprehensively the behaviour of a hip implant under dynamic conditions that simulate long-term use by a patient [13,16]. Displacement, rather than force, control was used. Consequently, “softening” of the hip implant with each subsequent load cycle caused a slight drift of the force level. Contributing issues may have been slippage of the femoral ball inside the steel pelvic cup and slippage of the cement block mounted in the industrial vice. Even so, the linearity of the force versus displacement graphs was $R^2 = 0.98$, indicating minimal influence from these factors.

Cyclic loading frequency was set to 5 Hz because a 3 to 5 Hz range is the minimum required by this IR thermography technology to be able to capture useful images. Normal human walking gait is often modelled in biomechanical studies using 1 to 3 Hz [13, 16]. Even so, the relative performance of the hip implant from low to medium to high cyclic forces would likely be similar at 1 to 3 Hz, although the absolute stress values would probably be lower at 1 to 3 Hz.

The composite hip implant was tested in isolation without being mounted proximally either in a cadaveric or synthetic femur, which would have been a more clinically realistic scenario. The quality of bone and bone-implant interfaces can influence load transfer from implant to bone and, hence, the resulting stress distribution [15, 20]. The rigid mounting of the current implant into a cement chamber, therefore, simulated perfect fixation in excellent bone stock. Blurry and low contrast images from thermography might have been due to suboptimal camera focusing,

environmental thermal noise, and surface texturing of the hip specimen. The two prior studies that used comparable technologies in a biomechanics application showed similar image quality [11-12]. Moreover, the geometry of the steel pelvic cup used to apply load to the femoral ball prevented adequate thermographic images from being taken on the medial side of the implant. Nonetheless, once images were examined in detail and the data extracted, stress values were virtually identical to those from strain gauges, indicating image reliability.

Linear strain gauges are thought not to work optimally on curved surfaces because they are ideally meant for flat surfaces to yield reliable strain values. Strain and stress gradients could be expected to change rapidly in such circumstances. Strain gauges also may peel or unglue easily when placed on textured surfaces, thereby giving unstable voltage signals and unstable strain results. The hip implant used in this study had both curved and textured surfaces which may have potentially influenced the results, yet there was almost perfect correlation between measurements made with IR thermography and strain gauges ($R^2 = 0.96$; slope = 1.01).

5. Conclusions

Lock-in IR thermography was used for non-destructive evaluation of a polymer composite hip implant. It yielded full three-dimensional stress maps and has potential use for other orthopaedic biomechanics applications. The current results were validated by strain gauge measurements.
The hip implant itself showed high peak stresses just distal to the neck region, which is a site for potential clinical failure. Surface stresses rose in direct proportion to the amount of axial cyclic load applied. This is the first study in the literature which has experimentally validated this lockin IR thermography technology in assessing an orthopaedic implant.

Remerciements
Special thanks to NSERC DG and St Michael's Hospital, Toronto, Canada

Références

[1]. L. Cristofoloni, « A critical analysis of stress shielding evaluation of hip prosthesis ». *Crit Rev Biomed Eng,* Vol. 25, pp. 409-483. 1997.
[2]. D. Berry, WS. Harmsen, ME. Cabanela, BF. Morrey. « Twenty- five-year survivorship of two thousand consecutive primary Charnley total hip replacements: Factors affecting survivor- ship of acetabular and femoral components ». *J Bone Joint Surg Am,* Vol. 84, pp. 171–177. 2002.
[3]. M. Akay, N. Aslan. « Numerical and experimental stress analysis of a polymeric composite hip joint prosthesis ». *J Biomed Mater Res* Vol. 31, pp. 167-182. 1996.
[4]. JA. Simões, AT. Marques. « Design of a composite hip femoral prosthesis ». *Mater Des,* Vol. 26, pp. 391–401. 2005.
[5]. H. Bougherara, M. Bureau, M. Campbell, A. Vadean, L. Yahia « Design of a biomimetic polymer composite hip prosthesis ». *J Biomed Mater Res Part A,*Vol.82, pp. 27-40. 2007.
[6]. H. Bougherara, R. Zdero, A. Dubov, S. Shah, S. Khurshid, EH. Schemitsch. « A preliminary biomechanical study of a novel carbon-fibre hip implant versus standard metallic hip implants ». *Med Eng Phys*, Vol. 33(1), pp. 121-128. 2011
[7]. S. Ramakrishna, J. Mayer, E. Wintermantel, KW. Leong. « Bio- medical applications ofpolymer-composite materials: A re- view ». *Compos Sci Technol,* Vol. 61, pp. 1189–1224. 2001.
[8]. M. Campbell, J. Denault, L. Yahia, MN. Bureau. « CF/PA12 composite femoral stems: Manufacturing and properties ». *Composites Part A*, Vol. 39, pp. 796-804. 2008.
[9]. S. Dimitrievska, J. Whitfield, SA. Hacking, MN. Bureau. « Novel carbon fiber composite for hip replacement with improved in vitro and in vivo osseointegration ». *J Biomed Mater Res - Part A,* Vol. 91, pp. 37-51. 2009.
[10]. R. Zdero, H. Bougherara. « Orthopaedic Biomechanics: A Practical Approach to Combining Mechanical Testing and Finite Element Analysis ». *chapter 7, In: Finite Element Analysis*, David Moratal, ed., Intech Education and Publishing, Vienna, 2010.
[11]. EM. Zanetti, SS. Musso, AL. Audenino. « Thermoelastic stress analysis by means of a standard thermocamera ». *Experimental Techniques*, March-April, pp. 41-50. 2007.
[12]. K. Hyodo, M. Inomoto, W. Ma, S. Miyakawa, T. Tateishi. « Thermoelastic stress imaging for experimental evaluation of hip prosthesis design ». *JSME International Journal: Series C*, Vol. 44(4), pp. 1065-1071. 2001.

[13]. G. Bergmann, F. Graichen, A. Rohlmann. « Hip joint loading during walking and running, measure in two patients. ». *J Biomech*, Vol. 26(8), pp. 969-990. 1993.

[14]. B. Helgason, H. Pálsson, TP. Rúnarsson, L. Frossard, M. Viceconti. « Risk of failure during gait for direct skeletal attachment of a femoral prosthesis: A finite element study ». *Med ng Phys*, Vol. 31, pp. 595-600. 2009.

[15]. H, Bougherara, R. Zdero, S. Shah, M. Miric, M. Papini, P. Zalzal, EH. Schemitsch, «A Biomechanical Assessment of Modular and Monoblock Revision Hip Implants using FE Analysis and Strain Gage Measurements ». *J Orthop Surg Res,* Vol. 12, pp. 5:34. 2010.

[16]. M. Talbot, R. Zdero, EH. Schemitsch. « Cyclic Loading of Periprosthetic Fracture Fixation Constructs ». *J Trauma,* Vol. 64(5), pp. 1308-1312. 2008.

[17]. M. Talbot, R. Zdero, D. Garneau, PA. Cole, EH. Schemitsch, « Fixation of long bone segmental defects: A biomechanical study ». *Injury*, Vol. 39, pp. 181-186. 2008.

[18]. R. Zdero, R. Walker, JP. Waddell, EH. Schemitsch. « Biomechanical Evaluation of Periprosthetic Femoral Fracture Fixation ». *J Bone Joint Surg Am*, Vol. 90(5), ppp. 1068-1077. 2008.

[19]. A. McConnell, R. Zdero, K. Syed, C. Peskun, EH. Schemitsch, « The Biomechanics of Ipsilateral Intertrochanteric and Femoral Shaft Fractures: A Comparison of 5 Fracture Fixation Techniques ». *J Orthop Trauma*, Vol. 22(8), pp. 517-524. 2008.

[20]. H. Bougherara, R. Zdero M. Miric, S. Shah, M. Hardisty, P. Zalzal, EH. Schemitsch. « The Biomechanics of the T2 Femoral Nailing System: A Comparison of Synthetic Femurs with Finite Element Analysis Proc Instn Mech Engrs (Part H) ». *J. Engineering in Medicine*, Vol. 223(H3), pp. 303-314. 2009.